A study of Fermi hole for some atomic systems

Khalil H. AL-Bayati * Kassem A. Mohammed **
Khalid O. AL-Baiti ***

Date of acceptance 28/5/2005

Abstract

The electron correlation effect for inter-shell can be described by evaluating the Fermi hole $\Delta f(r_{12})$ and partial Fermi hole $\Delta g(r_{12}, r_1)$ for Li atom comparing with Be^+ and B^{2+} ions (Li-Like ions) using the approximation of Hartree-Fock wavefunction. Each plot of the physical properties in this work is normalized to unity. All results are obtained numerically by using computer programs.

WAVEFUNCTION APPROXIMATION

The Hartree-Fock (HF) atomic wavefunctions are independent particle-model approximations to non-relativistic Schrodinger equation for stationary states. The single determinant can be written as the antisymmetrized product of all occupied HF spin-orbital for atoms .

$$\Phi_{HF}(1\,2\,3\ldots N) = A\,\Pi(1\,2\,3\ldots N) \quad \ldots(1)$$

Where A is the antisymmetrized operator given by [1]:

$$A = \frac{1}{\sqrt{N!}} \sum_{P} (-1)^{P}\, P \quad \ldots (2)$$

$(-1)^P$ takes the values +1 and −1 for even and odd permutation, P is any permutation of the electron, and the factor $\frac{1}{\sqrt{N!}}$ introduced to ensure that the wavefunction is normalized.

The product $\Pi(123\ldots N)$ in equation (1) can be defined as[2]:

$$\Pi(1\,2\,3\cdots N) = \phi_1(1)\,\phi_2(2)\,\phi_3(3)\cdots\phi_N(N) \quad \ldots\ldots(3)$$

The Hartree-Fock spin-orbital ϕ are designated by the numerals 1,2,3…N starting with the lowest orbital with spin. Consequently all odd integers for α spin and all even ones for β spin[3,4].

For our purpose the wavefunction can be written as

$$\Phi_{HF}(1\,2\,3\ldots N) = \sum_{i<j}^{N} A_{ij}^{mn} (-1)^{P}\, A\Pi_{ij} \quad \ldots\ldots\ldots(4)$$

* Dr.-Physics Dept.-College of Science for Women-University of Baghdad.
** Physics Dept.-College of Education (Ibn-AL-Haitham)-Baghdad University
*** Physics Dept.-College of Education (Ibn-AL-Haitham)-Baghdad University

Where the pair function A_{ij}^{mn} can be defined as [2]:

$$A_{ij}^{mn} = \phi_i(m)\phi_j(n) - \phi_j(m)\phi_i(n) \quad \text{.....(5)}$$

And Π_{ij} represents the product of all occupied HF-spin orbital except $\phi_i(m)$ and $\phi_j(n)$. i and j represent spin orbital labels, also m and n referred to electron labels.

Equation (1) can be expressed in the term of Slater determinant as follows[5]:

$$\Phi_{HF}(123\cdots N) = \frac{1}{\sqrt{N!}}\begin{vmatrix} \phi_1(1)\phi_1(2) & \cdots & \cdots & \phi_1(N) \\ \phi_2(1)\phi_2(2) & \cdots & \cdots & \phi_2(N) \\ \cdots & \cdots & \cdots & \cdots \\ \cdots & \cdots & \cdots & \cdots \\ \phi_N(1)\phi_N(2) & \cdots & \cdots & \phi_N(N) \end{vmatrix}$$

...(6)

The HF or analytic self-consistent field atomic wavefunction provided the uncorrelated description of each atom.

For any atom or ion, the Hartree-fock spatial orbital may be written as [6]:

$$\Phi = \sum_{i=1}^{j} c_i \chi_i$$

...(7)

Where c_i represents the constant coefficient yield from the SCF method to minimized the total energy.

And the basis function χ_i is the standard normalized Slater-type orbital (STO's) which given by:

$$\chi_{n\ell m}(r,\theta,\phi) = R_{n\ell}(r)Y_{\ell m}(\theta,\phi) \quad \text{.....(8)}$$

Where $R_{n\ell}(r)$ represented the radial part of the wavefunction and is given as:

$$R_{n\ell}(r) = N_{n\ell m}S_{n\ell}(r) \quad \text{.....(9)}$$

$N_{n\ell m}$ is The normalization constant and given as:

$$N_{n\ell m} = \frac{(2\zeta)^{n+\frac{1}{2}}}{[(2n)!]^{\frac{1}{2}}}$$

...(10)

and

$$S_{n\ell}(r) = r^{n-1}e^{-(\zeta r)}$$

...(11)

where $S_{n\ell}(r)$ is called Slater type orbital (STO's).

and $Y_{\ell m}(\theta,\phi)$ represented the angular part of the wavefunction.

Fermi hole calculations

In this work we will calculate the Fermi hole $\Delta f(r_{12})$ and the partial Fermi hole $\Delta g(r_{12}, r_1)$ for Li-like ion

The two-density function $\Gamma_{ij}(r_1, r_2)$ for Li-like ions can be expressed for the singlet state inter-shell $KL(^1S)$ after integrated over all spins and angular functions as:

$$\Gamma_{KL(^1S)}(r_1, r_2) = \frac{1}{2}\left[R_{1s}^2(r_1)R_{2s}^2(r_2) + R_{2s}^2(r_1)R_{1s}^2(r_2)\right]$$

...(12)

and for the triplet state inter-shell $KL(^3S)$:

$$\Gamma_{KL(^3S)}(r_1,r_2) = \frac{1}{2}\left[\begin{array}{l} R^2_{1s}(r_1)R^2_{2s}(r_2) + \\ R^2_{2s}(r_1)R^2_{1s}(r_2) - 2R_{1s}(r_1)R_{2s}(r_1)R_{1s}(r_2)R_{2s}(r_2)\end{array}\right]$$

.. (13)

(1)Calculation method of Fermi hole $\Delta f(r_{12})$:

Fermi hole can be defined as a difference between the inter-particle distribution function $f(r_{12})$ for triplet state $KL\ (^3S)$ and singlet state $KL\ (^1S)$.

$$\Delta f(r_{12}) = f_{KL(^3S)}(r_{12}) - f_{KL(^1S)}(r_{12})$$

.....(14)

$f(r_{12})$ for the both states for Li-Like ions can be written as [7] :

$$f(r_{12}) = 0.5 r_{12}\left[\begin{array}{l} \int_{r_{12}}^{\infty} r_1 dr_1 \int_{r_1-r_{12}}^{r_1+r_{12}} \Gamma(r_1,r_2) r_2 dr_2 \\ + \int_0^{r_{12}} r_1 dr_1 \int_{r_{12}-r_1}^{r_{12}+r_1} \Gamma(r_1,r_2) r_2 dr_2 \end{array}\right]$$

..(15)

2 Calculation method of partial Fermi hole $\Delta g(r_{12},r_1)$:

Following the definition of Fermi hole, the partial Fermi hole is defined as a difference between the partial distribution function $g(r_{12},r_1)$ for triplet state $KL\ (^3S)$ and singlet state $KL\ (^1S)$.

$$\Delta g(r_{12},r_1) = g_{KL(^3S)}(r_{12},r_1) - g_{KL(^1S)}(r_{12},r_1)$$

...(16)

The partial distribution function $g(r_{12},r_1)$ for the both state for Li-Like can be calculated as following[8]:

$$g_{KL(^1S)}(r_{12},r_1) = 0.5 r_1 r_{12} \int_{|r_1-r_{12}|}^{r_1+r_{12}} \Gamma(r_1,r_2) r_2 dr_2$$

.(17)

RESULTS, DISCUSSION AND CONCLUSION

(1) Fermi hole $\Delta f_{(r_{12})}$ results and discussion :

The probability of finding the inter-particle distribution function $f(r_{12})$ between electrons unlike and like spins in KL shell for Li-Like ions can be observed in the curves (A) and (B) presented in fig.(1),fig.(3) and fig.(5) for Z=3,4 and 5 respectively. At small r_{12} the $f(r_{12})$ distribution function will be influenced mainly by the electron pair behavior when the outer electron has penetrated the K-shell. For the $KL(^3S)$ curve, the existence of Fermi effect produces a flat region at small r_{12} whereas, by marked contrast, the $KL(^1S)$ curve is seen to possess a small local maximum. Clearly, when the K-and L-shell electrons have different spin assignments but are both described by orbitals of s-type symmetry, a double occupancy can occur in the K-shell region. The maximum values and their locations of the density distribution function max$f(r_{12})$ are tabulated in table (1) of curves A and B which are presented in fig.(7). This figure shows as Z increases, the maximum probabilities of the inter-particle density distribution function $f(r_{12})$ for singlet and triplet state are increasing

and they are observed that the locations of these maxima decrease as Z become large.Fermi hole is plotted as a difference between $f(r_{12})$ of $KL(^3S)$ shell (triplet state) and shell $KL(^1S)$ shell (singlet state)for a series of Z for Li-Like ions in fig.(2), fig.(4) and fig.(6). Inspection of fig.(8) which shows as Z increases, the radius of Fermi hole decreases and it is observed that the depth of Fermi hole increases as Z become large, all that because the nuclear charge is increasing. The radius and the area of the holes for groups of Li are tabulated in table (2).

(2)The partial Fermi hole $\Delta g(r_{12},r_1)$ results and discussion:

The $g(r_{12},r_1)$ diagrams (surfaces and contours) for $KL(^1S)$-and $KL(^3S)$-shells for group Li-Like ions presented in figs.(9,10,11,12),show the change in behavior of the inter-particle probability functions as the position of the test electron is varied . These surfaces have their main characteristics located about the $r_{12} = r_1$ diagonal line and parallel to the r_{12} axis for small r_1 . In addition, and as expected, when Z increases the pattern contracts towards the origin and the magnitude of these densities increases. The diagonal distribution is again asymmetric with the $r_{12} = r_1$ axis: the maximum is always slightly on the right hand side (RHS) of $r_{12} = r_1$ axis for any selected and fixed r_1 value outside the K-shell.From the comparison between the $g(r_{12},r_1)$ surfaces and Contours for the $KL(^1S)$- and $KL(^3S)$ - shells, it can be seen that a difference exists only at $r_{12} = r_1 \approx r_k$. Since there is no Fermi effect in $KL(^1S)$,it can also be seen that the removal of mini K-shell density causes the main characteristics to move towards the origin slightly.The contour diagrams shows that the $g(r_{12},r_1)$ becomes more diffuses and decreases in magnitude as Z increases for Li iso electronic sequences .The locations and the maximum values of the partial density distribution function $g(r_{12},r_1)$ when r_1 fixed and r_{12} is varied then r_{12} fixed and r_1 is varied of $KL(^1S)$ and $KL(^3S)$ for the Li-like ions are tabulated in table (3).

A partial Fermi hole as a difference between triplet state $KL(^3S)$ and singlet state $KL(^1S)$ is plotted as a surface diagrams of the series of Z in the fig.(13) for Li-Like ions. And it is plotted as a contour diagrams of the series of Z in the fig.(14) for Li-Like ions. The surface diagrams shows that the depth of partial Fermi hole is increases and the radius is decreases as Z increasing and the contour diagrams shows a Fermi hole becomes more diffuses and decreases in magnitude as Z increases. The size of the partial Fermi hole, as presented in the fig.(15) and fig.(16), can be studied clearly by the surface and the contour diagrams for Li-Like ions.

Conclusions

From the present work, we deduce some notes for some atomic properties and Fermi hole and Coulomb hole.

1. Due to the Fermi effect, the $f(r_{12})$ for the $KL(^3S)$ -shell gives a flat region at small r_{12} and this result approves the definition of Fermi hole whereas, the result for the $KL(^1S)$ -shell do not exhibit a flat region due to a Coulomb repulsion between unlike spin orbitals.
2. As Z increases, the maximum probabilities of the inter-particle distribution function $f(r_{12})$ for singlet and triplet state increases and also the locations of these maxima decreases as Z increases.
3. The magnitude density of $g(r_{12},r_1)$ for singlet and triplet state increases as Z increases.

4. The radius of Fermi hole decreases and the depth of Fermi hole increase as Z increases.
5. As Z increases, the depth of partial Fermi hole increases and the radius decreases.

Table (1) The locations and the maximum values of the inter-particle density distribution function $f(r_{12})$ for the Li-like ions.

Atom or Ion	Shell	r_{12}	$f(r_{12})$
Li	KL(^{1}s)	0.5	0.016924
		3.2	0.26752
	KL(^{3}s)	3.2	0.26634
Be^+	KL(^{1}s)	0.4	0.044626
		2.0	0.462221
	KL(^{3}s)	1.9	0.460295
B^{2+}	KL(^{1}s)	0.3	0.073301
		1.4	0.64674
	KL(^{3}s)	1.4	0.64557

Table (2) the radius and the area of Fermi hole $4\gamma_r(r_{12})$ using Hartree-Fock approximation for Li-Like ions.

$4f_r(r_{12})$		
Atom or Ion	Radius r_{12} = a.u	Area of Fermi hole
Li	0.935	0.009648
Be^+	0.658	0.017342
B^{2+}	0.510	0.023964

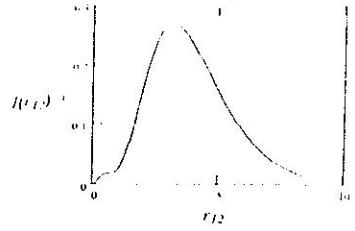

(A)

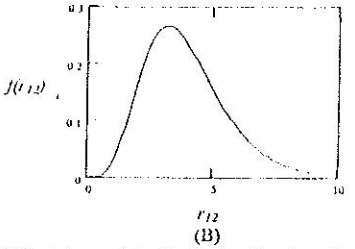

(B)

Fig.(1) The inter-particle distribution function $f(r_{12})$ for Li atom
(A) $KL(^1S)$ (B) $KL(^3S)$

Table (3) The locations and the maximam values of the partial density distribution function $g(r_{12},r_1)$ for HF wavefunction, when r_1 fixed and r_{12} is varied then r_{12} fixed and r_1 is varied for the Li-like ions.

atom or	Shell	when r_1 is fixed			when r_{12} is fixed		
		r_1	r_{12}	$g(r_{12},r_1)$	r_{12}	r_1	$K(r_{12},r_1)$
Li	KL(^{1}S)	0.36	3.1	0.19118	3.2	0.36	0.19097
	KL(^{3}S)	0.35	3.1	0.19235	3.2	0.36	0.19207
Be^+	KL(^{1}S)	0.28	1.9	0.46188	2.0	0.26	0.46008
	KL(^{3}S)	0.25	3.1	0.17191	1.9	0.35	0.11711
B^{2+}	KL(^{1}S)	0.20	1.5	0.58092	1.4	0.22	0.8313
	KL(^{3}S)	0.20	3.0	0.14603	1.4	0.34	0.056699

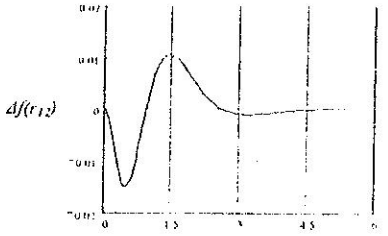

Fig.(2) Fermi hole as a difference between the inter-particle distribution function $f(r_{12})$ for Li atom

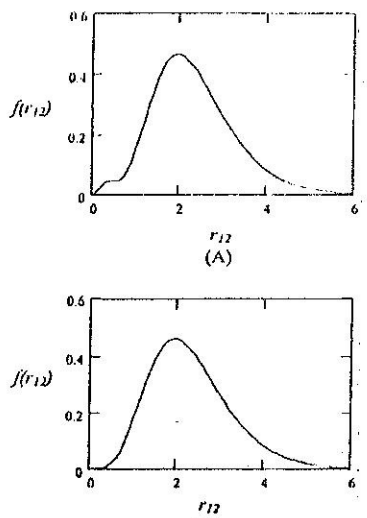

Fig.(3) The inter-particle distribution function $f(r_{12})$ for Be^+ ion
(A) $KL(^1S)$ (B) $KL(^3S)$

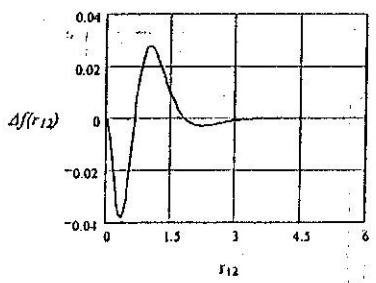

Fig.(4) Fermi hole as a difference between the inter-particle distribution function $f(r_{12})$ for Be^+ ion

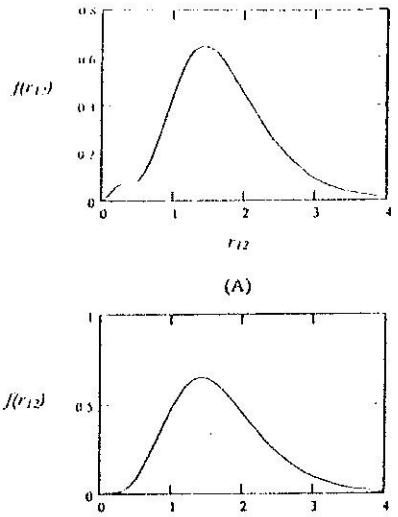

Fig.(5) The inter-particle distribution function $f(r_{12})$ for B^{2+} ion
(A) $KL(^1S)$ (B) $KL(^3S)$

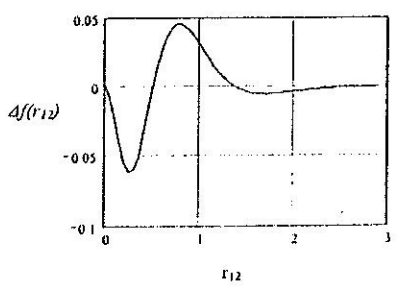

Fig.(6) Fermi hole as a difference between the inter-particle distribution function $f(r_{12})$ for B^{2+} ion

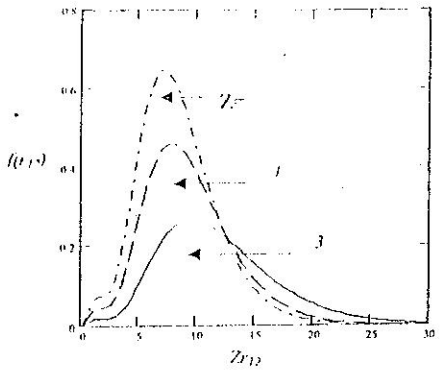

(A)

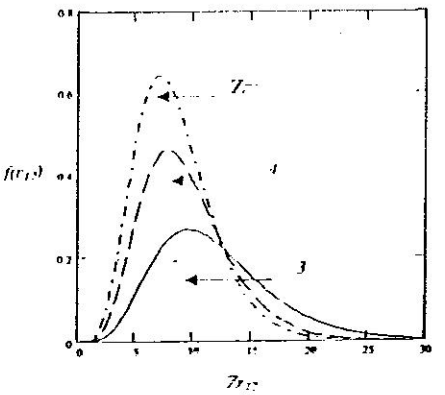

(B)

Fig.(7) The inter-particle distribution function $f(r_{12})$ for Li atom,Be^{+} ion and B^{2+} ion
(A) $KL(^1S)$ (B) $KL(^3S)$

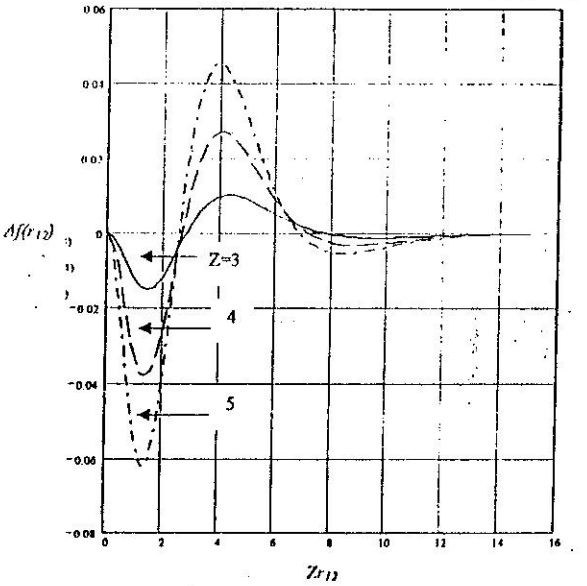

Fig.(8) Fermi hole as a difference between the inter-particle distribution function $f(r_{12})$ of $KL(^3S)$ and $KL(^1S)$ for Li atom,Be^{+} ion and B^{2+} ion

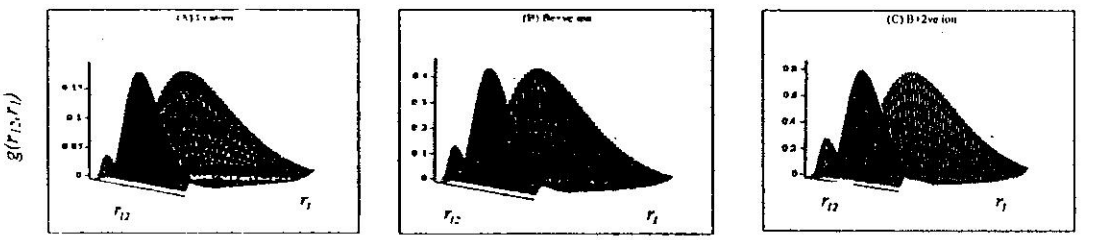

Fig.(4-9) The Surfaces of the partial distribution function $g(r_{12},r_1)$ of $KL\ (^1S)$ for
(A) Li atom (B) Be^{+} ion (C) B^{2+} ion

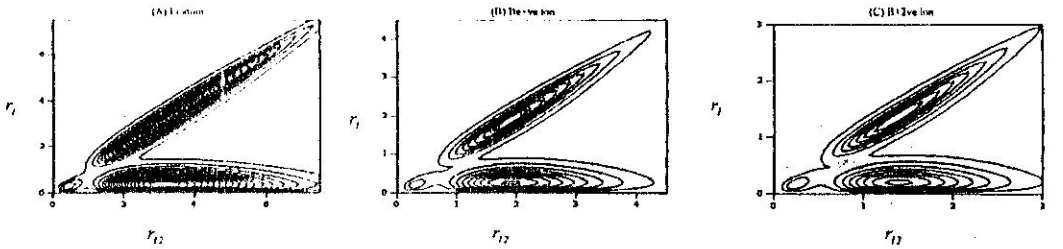

Fig.(4-10) The Contours of the partial distribution function $g(r_{12},r_1)$ of $KL\ (^1S)$ for
(A) Li atom (B) Be^{+} ion (C) B^{2+} ion

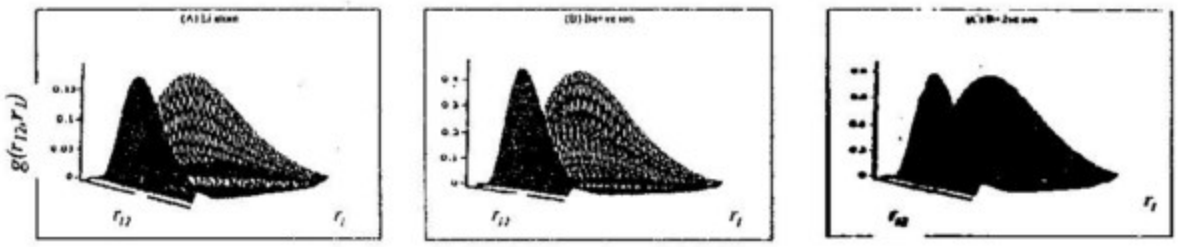

Fig.(4-11) The Surfaces of the partial distribution function $g(r_{12},r_1)$ of KL (^{3}S) for
(A) Li atom (B) Be$^+$ ion (C) B^{2+} ion

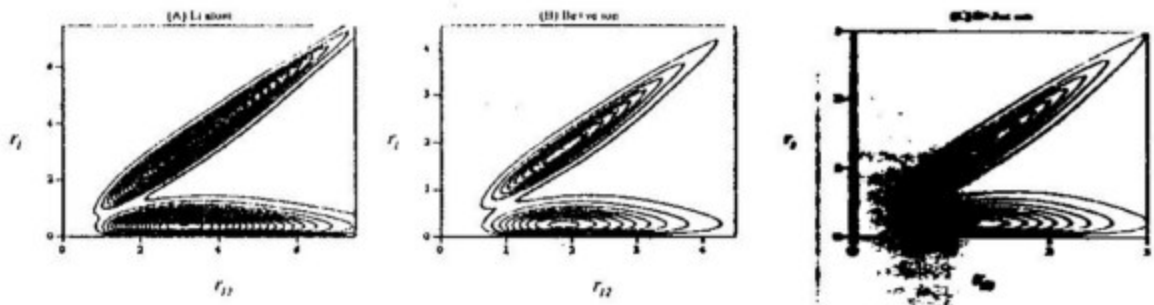

Fig.(4-12) The Contours of the partial distribution function
(A) Li atom (B) Be$^+$ ion (C) B^{2+} ion

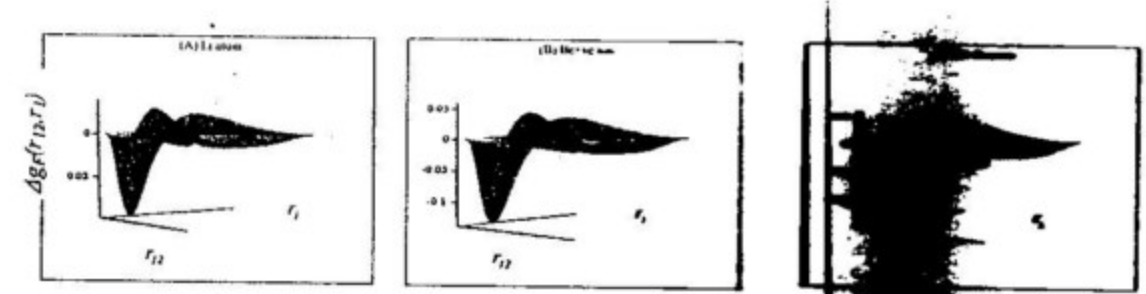

Fig.(4-13) The Surfaces of the partial Fermi hole as a difference between
of KI (^{3}S) and KL (^{3}S) for
(A) Li atom (B) Be$^+$ ion

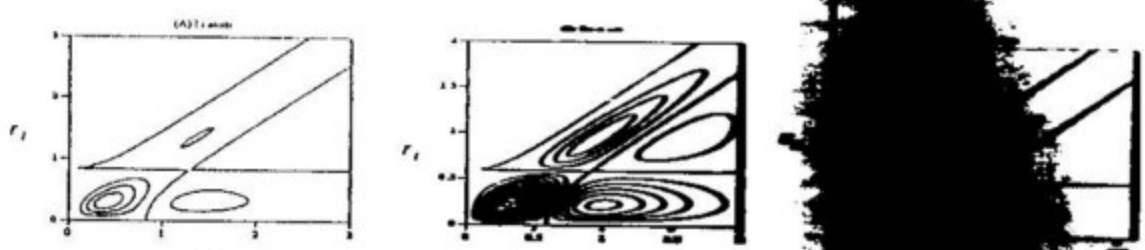

Fig.(4-14) The Contours of the partial Fermi hole as a difference between
of KL (^{3}S) and KL (^{3}S) for
(A) Li atom

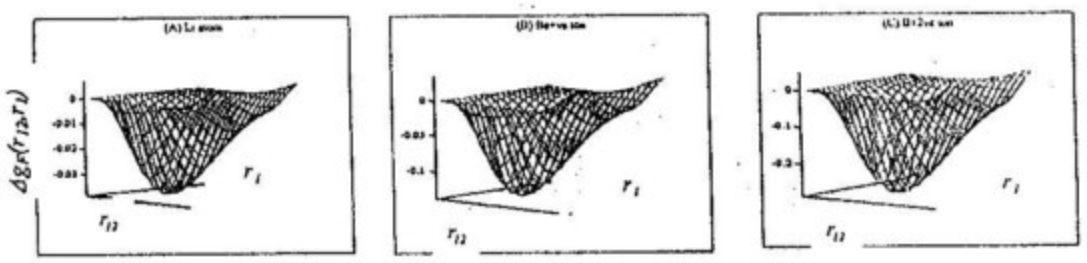

Fig.(4-*f*) The surfaces of the size of partial Fermi hole as a difference between the partial distribution function $g(r_{12},r_1)$ of $KL\ (^3S)$ and $KL\ (^1S)$ for
(A) Li atom (B) Be^+ Ion (C) B^{2+} Ion

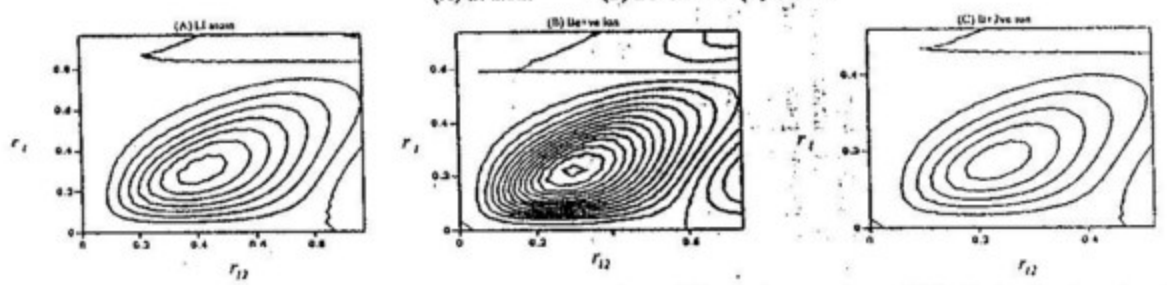

Fig.(4-*f*) The Contours of the size of partial Fermi hole as a difference between the partial distribution function $g(r_{12},r_1)$ of $KL\ (^3S)$ and $KL\ (^1S)$ for
(A) Li atom (B) Be^+ ion (C) B^{2+} ion

References

1. Sims, J. S. and S. A. Hagstrom,1975 Combined configuration – interaction – Hylleraas studies of atomic states. .Physical Review A,Vol.11,No.2,P. 418.
2. Al-Bayati, K.H..Um.Salama Science ournal, ollege f cience for Women,University of Baghdad-Vol.2Year 2004. Evaluation of the one-electron expectation values for different wave functions
3. Weiss, A.W1963 wavefunctions and oscillator strengths for the Lithium isoelectronic sequence , J . Chem.Phys.,39,1262
4. Clementi and C.Roetti, E. 1974 Atomic Data and Nuclear Data 14,177
5. Johnson, W.R. 2002 "Lecture on Atomic Physics", Department of physics university of Notredam, Notredam, Indiana, U.S.A..
6. Bunge,C.F. J.A. Barrientos And A.V. Bunge, 1993 Roothaan – Hartree – Fock ground – state atomic wave function,Atom. Data Nucl. Data Tables, 53,133 .
7. Coulson and A.H.Neilson, C. A. 1961 Electron Correlation in the Ground state of Helium. Proc. Phys. Soc., 78,831.
8. AL-Bayati, K. H. 1984 Electron correlation in the $(1s^2\ 2s\ )^2S$ and $(1s^2\ 2p)^2P$ states of the Lithium isoelectronic sequence in position and momentum space. PhD. Thesis, Leicester University, England.

دراسة فجوة فيرمي لبعض الأنظمة الذرية

*خليل هادي البياتي **قاسم عزيز محمد **خالد البيت

*قسم الفيزياء- كلية العلوم للبنات-جامعة بغداد
**قسم الفيزياء- كلية التربية ابن الهيثم-جامعة بغداد

الخلاصة

تأثير الرابطة الالكترونية للمدار البيني يمكن دراسته بواسطة فجوة فيرمي $\Delta f(r_{12})$ و فجوة فيرمي الجزئية $\Delta g(r_{12},r_1)$ لذرة الليثيوم Li مقارنة مع ايونات Be^{+} , B^{+2} (ايونات المشابهة لليثيوم Li) باستخدام الدالة الموجية لهارتري فوك التقريبية كل رسم للخصائص الفيزياوية في هذا العمل يحقق شرط المعيارية للواحد كل النتائج تم حسابها عدديا باستخدام برامج حاسوبية

** حاليا تدريسي في جامعة حضرموت - اليمن